Preprint
UCRL-ID-141467

Implicit Monte Carlo Diffusion – An Acceleration Method for Monte Carlo Time Dependent Radiative Transfer Simulations

N. A. Gentile

This article was submitted to Nuclear Explosives Code Developers Conference, October 23-27, 2000, Oakland, California

October 1, 2000

DISCLAIMER

Implicit Monte Carlo Diffusion - An Acceleration Method for Monte Carlo Time Dependent Radiative Transfer Simulations (U)

N. A. Gentile
Lawrence Livermore National Laboratory

abstract

We present a method for accelerating time dependent Monte Carlo radiative transfer calculations by using a discretization of the diffusion equation to calculate probabilities that are used to advance particles in regions with small mean free path. The method is demonstrated on problems with on 1 and 2 dimensional orthogonal grids. It results in decreases in run time of more than an order of magnitude on these problems, while producing answers with accuracy comparable to pure IMC simulations. We call the method Implicit Monte Carlo Diffusion, which we abbreviate IMD. (U)

Introduction

The time dependent transport equation for gray photons in the absence of scattering is (Pomraning, 1983)

$$\frac{1}{c}\frac{\partial I}{\partial t} + \hat{\Omega}\cdot\nabla I = -\sigma_a I + c\sigma_a a T^4 \tag{1}$$

where c is the speed of light, σ_a is the macroscopic absorption cross section in inverse length units and T is the matter temperature. The transport equation is coupled to the material energy balance equation (Pomraning,1983)

$$\frac{\partial E_m}{\partial t} = c\sigma_a \int I \mathrm{d}\Omega - c\sigma_a a T^4 \tag{2}$$

Here, E_m is the matter energy density in units of energy per volume. These equations can be solved by a Monte Carlo method described (Fleck, 1963). The method discetizes the problem on a mesh. Each zone has a temperature and absorption and scattering cross sections. Particles representing photons are created in the zones at the beginning of each time step according to the emission term in the transport equation. Then the photons are followed through the zones, heating them according to the absorption term in Eq.(1). The zone temperatures are updated at the end of the time step, and the process is repeated.

This work was performed under the auspices of the U.S. Department of Energy by the University of California Lawrence Livermore National Laboratory under contract No. W-7405-Eng-48.

This method becomes unstable when time steps of the order of (FLeck and Cummings,1971)

$$\Delta t = \frac{\rho c_v}{aT^3 c\sigma_P} \tag{3}$$

are taken. Here ρ is the density of the matter, c_v is the specific heat capacity in units of energy per mass per temperature, and σ_P is the Planck mean opacity in inverse length units. This instability occurs when the matter and radiation fields exchange an amount of energy comparable to the amount of energy necessary to change the matter temperature a non-negligible amount in one time step. If the matter is only able to absorb energy during a time step, but is not able to reradiate, as in the algorithm in (Fleck, 1963), then instabilities will occur. The inability of the matter to re-radiate the energy it absorbs from the radiation during a time step is related to the fact that the temperature in the emission term of the transport equation is calculated using the temperature at the beginning of the time step.

A method providing unconditional stability for the photon transport equation was provided by Fleck and Cummings (FLeck and Cummings,1971). The method was dubbed Implicit Monte Carlo, usually abbreviated IMC. IMC works by using the matter energy balance equation to estimate the future matter temperature, and using this estimate in the transport equation. This substitution has the effect of reducing the absorption opacity in the transport equation by a factor of

$$f = \frac{1}{1 + \beta c \Delta t \sigma_P} \tag{4}$$

and adding an amount of thermally redistributed isotropic scattering. Here $\beta = aT^3/\rho c_v$.

The factor f is small when photons are being absorbed and quickly re-emitted by the matter. Problems in which this occurs are said to exhibit tight coupling between the radiation and matter. IMC replaces the absorption and rapid reemission occurring in tightly coupled problems with isotropic scattering. This scattering is usually referred to as the induced scattering, to distinguish it from physical scattering. The induced scattering $\sigma_s = (1 - f)\sigma_a$.

When the scattering, either physical or induced, is large, then the mean free path of photons can be much smaller than a typical dimension of the zones in the discretized mesh. IMC particles take many steps in these zone. Each simulated photon path in an IMC calculation is about equally expensive; thus, simulations with a large scattering cross section can be very time consuming to calculate. The end result of applying the IMC algorithm is to stabilize the calculation, at the cost of making highly absorbing, tightly coupled problems as expensive to run as highly scattering ones.

When a problem has a large cross section for isotropic scattering, a numerical solution of the diffusion equation can provide a more rapid solution technique (Pomraning,1983). The diffusion equation describes the time development of the radiation energy density, which is the zeroth moment of the intensity I :

$$\frac{\partial E}{\partial t} + \nabla \cdot F = c\sigma_a aT^4 - c\sigma_a E \tag{5}$$

Where E, the radiation energy density , is defined by

$$E = \int I \mathrm{d}\Omega \tag{6}$$

and the flux F, the first moment of I is defined by

$$F = \int \hat{\Omega} I \mathrm{d}\Omega. \tag{7}$$

To allow us to calculate E from this equation, we must define F in terms of E. This is usually done by using Fick's law:

$$F = -cD\nabla E \tag{8}$$

where $D = 1/(3\sigma)$ is the diffusion coefficient.

The diffusion equation can be derived from the transport equation by taking moments of the transport equation, and taking the limit as the factor (Larsen,1980)

$$\epsilon = \frac{\sigma^{-1}}{L} = \frac{mean\ free\ path}{characteristic\ length\ of\ the\ flux} \tag{9}$$

becomes small. Thus, the solution of the diffusion equation is an accurate approximation to the first moment of the solution of the transport equation when the intensity describes photons with a nearly isotropic angular distribution which is slowly varying in space and time. Thus, the diffusion equation can provide an accurate approximation for highly scattering problems where IMC is prohibitively expensive.

Since IMC is expensive where diffusion is accurate, solution techniques have been developed that employ IMC in parts of the problem with a small induced scattering and some form of diffusion in parts of the problem with a large induced scattering (Pomraning and Foglesong, 1979). These are referred to as hybrid methods.

A hybrid technique involves solving the diffusion equation on parts of the grid and IMC on other parts. The IMC simulation provides a flux that is used as a boundary condition for the solution of the diffusion equation, which usually requires a matrix inversion. The flux of energy out of the diffusion equation is turned into particles used by the IMC in the next time step.

A drawback to this method arises from problems in the coupling of the diffusion equation to the transport equation. The boundary condition of the diffusion equation is a net flux, while the boundary condition of the transport equation is an incoming flux. Using the diffusion equation to get a boundary condition from for the IMC may result in a negative energy flow (i.e., a negative number of particles) into the IMC, which is a difficulty for Monte Carlo calculations.

Our hybrid scheme avoids this. Using the matrix resulting from discretizing the diffusion equation in the highly scattering part of the problem, we derive probabilities for the Monte Carlo particles to deposit energy, reach census, or jump to another zone. Since this method involves a Monte Carlo solution of the diffusion equation, and uses the same stabilization technique as IMC, we have dubbed it Implicit Monte Carlo Diffusion, which we abbreviate IMD.

The IMD particle can jump to a new zone in one step, rather than taking many IMC steps. Our method in effect rolls many expensive IMC steps into one very cheap IMD step. Thus the calculation proceeds much more rapidly in the diffusion region than it would if we employed IMC there. Monte Carlo particles can freely cross the boundary from the diffusion region to the IMC region, and so no problems with negative energy flows result. Since the IMC particles can be run in the diffusive region, the two regions are coupled together implicitly, and no time step restrictions arise.

In the following sections, we develop the IMD algorithm and show how to make a hybrid IMC/IMD method. In section 2, we describe the discretization of the diffusion equation. In section 3, we show how to solve the matrix equation obtained by this discretization by a Monte Carlo method which resembles IMC. In section 4, we describe how to use the Monte Carlo diffusion method with IMC in a hybrid method. In section 5, we apply this hybrid method to various gray opacity test problems. We show that it can be considerably faster than IMC alone on problems with very opaque regions, while yielding a similar result.

Discretizing the Diffusion Equation

We will begin by considering the diffusion equation in Cartesian coordinates, In a 1 D slab geometry, as outlined in Szilard and Pomraning (1992). Our development will rely heavily on this derivation. The diffusion equation under these assumptions is (Szilard and Pomraning,1992)

$$\frac{1}{c}\frac{\partial E}{\partial t} - \frac{\partial}{\partial x}\left[D\frac{\partial E}{\partial x}\right] = \sigma_a a T^4 - \sigma_a E. \tag{10}$$

We will solve this equation by discretizing it as in Szilard and Pomraning (1992). We will take E to be a zone centered variable, and use backward Euler time differencing. The result is

$$\frac{1}{c}\frac{E_j^{n+1} - E_j^n}{\Delta t} - \frac{F_{j+1/2}^{n+1} - F_{j-1/2}^{n+1}}{\Delta x_j} = \sigma_{a\,j}(aT_j^{n4} + E_j^n). \tag{11}$$

Here j is a zone index, and j+(-)1/2 indicates the face in the increasing(decreasing) x direction.

In zones with neighbors, we can get F at the edges by discretizing Fick's law:

$$F_{j+1/2}^{n+1} = cD_{j+1/2}\frac{E_{j+1}^{n+1} - E_j^{n+1}}{\Delta x_{j+1/2}} \tag{12}$$

where

$$D_{j+1/2} = 2\Delta x_{j+1/2}\left[\frac{D_j D_{j+1}}{D_j \Delta x_{j+1} + D_{j+1}\Delta x_j}\right] \tag{13}$$

and

$$\Delta x_{j+12} = (\Delta x_j + \Delta x_{j+1})/2. \tag{14}$$

(As noted in in Szilard and Pomraning (1992), the harmonic average given in Eq.(13) will yield a small value for the face diffusion coefficient in cases where either zone has a small diffusion coefficient. This can occur in problems with temperature dependent opacities that are large in cold matter. A small diffusion coefficient leads to a small flux via Eq.(12); thus , the diffusion of heat into cold, opaque material may be unphysically retarded. In Szilard and Pomraning (1992), a means of dealing with this problem is outlined: essentially, the values of D employed in face calculations such as Eq.(13) are calculated using a common temperature derived from the temperatures of the neighboring zones. In this paper, this issue does not arise, because we have run only simulations with a temperature independent opacities.)

For the two edges at the ends of the problem, we get F from the boundary condition given in Szilard and Pomraning (1992)

$$F = \frac{c}{4}\left[E + 2D\hat{n}\cdot\nabla E\right]. \tag{15}$$

We should note an issue, described in Szilard and Pomraning (1992), that arises in the calculation of the diffusion coefficient D. This is the use of a flux limiter to prevent superluminal energy transport in regions with a small opacity. Several flux limiters and their effects are considered in Olson (2000).

The source term in Eq.(11) depends on the current matter temperature T_j^n, rather than the future matter temperature T_j^{n+1}, which would make the time differencing fully implicit. This can effect the quality of the solution, as discussed in Szilard and Pomraning (1992). This dependence on the current matter temperature rather than the future matter temperature is what led to the time step restriction Eq.(3) in the Monte Carlo solution of the transport equation.

This problem is addressed in Szilard and Pomraning (1992) by iterating on the matter temperature, but that requires multiple matrix inversions per time step. Instead, we choose to solve it in the same manner that is employed to stabilize the IMC algorithm. Solving the matter temperature equation to get an estimate of the future matter temperature, and using that in Eq.(10) yields

$$\frac{1}{c}\frac{\partial E}{\partial t} - \frac{\partial}{\partial x}\left[D\frac{\partial E}{\partial x}\right] = f\sigma_a aT^4 - f\sigma_a E \tag{16}$$

where f is the same factor, given Eq.(4), that is employed in IMC. As in IMC, this transformation results in induced isotropic scattering, which shows up in the diffusion coefficient. Since D is defined in terms of the sum of the opacities, it's value remains unchanged.

This transformed diffusion equation could also have been derived by starting with the transport equation as modified by IMC, integrating over angle, and applying Fick's law. This derivation would parallel the one in (Larsen,1980) with a factor of f modifying σ_a everywhere and a scattering opacity of $(1-f)\sigma_a$ in the transport equation.

Substituting in the definitions of the flux in terms of the energy into the discretized diffusion equation Eq.(11), and decreasing the absorption opacity by the factor f as in Eq.(16), we get

$$\left[1 + c\Delta t f_j \sigma_{a\,j} + c\frac{\Delta t}{\Delta x_j}\frac{D_{j-1/2}}{\Delta x_{j-1/2}} + c\frac{\Delta t}{\Delta x_j}\frac{D_{j+1/2}}{\Delta x_{j+1/2}}\right] E_j^{n+1}$$

$$-c\frac{\Delta t}{\Delta x_j}\frac{D_{j-1/2}}{\Delta x_{j-1/2}}E_{j-1}^{n+1} - c\frac{\Delta t}{\Delta x_j}\frac{D_{j+1/2}}{\Delta x_{j+1/2}}E_{j+1}^{n+1} = c\Delta t f\sigma_{a\,j}aT_j^{n4} + E_j^n. \tag{17}$$

At the $x = 0$ boundary, we get a similar equation relating E_1^{n+1} and E_2^{n+1} by differencing the flux given in Eq.(15) and inserting the result into Eq.(11). The result is

$$\left[1 + c\Delta t f_1\sigma_{a\,1} + c\frac{\Delta t}{\Delta x_1}\frac{3/2D_1\sigma_{a\,1}}{1+3\Delta x_1\sigma_{a\,1}/4} + c\frac{\Delta t}{\Delta x_j}\frac{D_{3/2}}{\Delta x_{3/2}}\right]E_1^{n+1}$$
$$-c\frac{\Delta t}{\Delta x_1}\frac{D_{3/2}}{\Delta x_{3/2}}E_2^{n+1} = c\Delta t f\sigma_a aT_1^{n4} + E_1^n + 4\left[\frac{3/2D_1\sigma_{a\,1}}{1+3\Delta x_1\sigma_{a\,1}/4}\right]\frac{F_0}{c\Delta x_1}. \tag{18}$$

In this equation, F_0 is the flux through the boundary at $x = 0$, which adds energy into the source term in zone 1. A similar equation is obtained at the $x = x_{max}$ end of the problem.

The equations defining E_j^{n+1} in terms of the neighboring values E_{j+1}^{n+1} and E_{j-1}^{n+1} the boundary fluxes is a matrix equation $Ax = b$, with the E_j^{n+1} the components of x and the source terms the components of b. The matrix A is tridiagonal and can easily be solved by standard techniques (Press, et.al., 1992) Below, we will outline a Monte Carlo technique for solving it.

In a manner similar to that applied above, we can get a matrix equation for a zone centered discretization of the diffusion equation in cylindrical coordinates in a 2 D axially symmetric geometry on an orthogonal mesh. Employing the usual five point differencing scheme results in a similar set of equations which has five off-diagonal bands.

In both the Cartesian 1D and the orthogonal cylindrical case, the matter energy density satisfies the same equation:

$$\frac{\partial E_m}{\partial t} = cf\sigma_a\int I\mathrm{d}\Omega - cf\sigma_a aT^4. \tag{19}$$

This is the same equation satisfied by the matter energy density in the IMC formulation.

The change in the matter energy density given by Eq.(19) is the difference between the energy thermally radiated by the matter and the energy absorbed from the radiation field. Often this equation is solved by introducing the heat capacity and writing

$$\rho c_v\frac{\partial T}{\partial t} = cf\sigma_a\int I\mathrm{d}\Omega - cf\sigma_a aT^4 \tag{20}$$

which can be differenced and solved for the temperature if c_v is assumed constant. This difference equation only conserves energy if c_v is actually constant. We prefer to difference Eq.(19) as

$$E_{m\,j}^{n+1} = E_{m\,j}^n + \Delta t\left[E_{absorbed\,j} - cf_j\sigma_{a\,j}aT_j^{n4}\right] \tag{21}$$

where $E_{absorbed\,j}$ is the amount of energy absorbed by the matter from the radiation field and is obtained from the solution of the diffusion equation.

Using Eq.(21), $E_{m\,j}^{n+1}$ is solved for the new matter energy at t^{n+1}, which can be numerically inverted using the equation of state to obtain the new matter temperature T^{n+1}.

Solving the Discretized Diffusion Equation by a Monte Carlo Technique

The matrix equations arising from the discretizations of the 1D Cartesian and 2D orthogonal cylyndrical diffusion equation are similar. In both cases, the diagonal element consists of the sum of the following terms: 1, arising from the time derivative term, $c\Delta t f \sigma_a$, arising from the absorption term, and several terms, one for each neighboring zone, involving the diffusion coefficient and geometric factors, which arise from the flux term. The off-diagonal elements are the negative of these diffusion coefficient terms. Both matrixes are diagonally dominant, and symmetric, and hence are symmetric positive definite.

The source terms are the same in both cases, consisting of the sum of the old energy density in the zone E_j^n and a source term depending on the temperature, $c\Delta t f \sigma_a a T^4$.

Here, we will derive a Monte Carlo solution technique that is applicable to both the 1D and 2D discretized diffusion equation (and is in fact applicable to any symmetric matrix equation in which the diagonal is of the opposite sign as the off diagonal terms.) Our derivation will employ the Eq.(16) above, but the generalization to the 2D case, and other matrixes, will be clear. If we take the matrix equation defined by Eq.(17) and solve it for E_j^{n+1} we obtain the following relation which defines the radiation energy density in zone j in terms of the radiation energy density of neighboring zones and the energy of the source in zone j:

$$E_j^{n+1} = E_{j-1}^{n+1} \hat{f}_{j-1/2} + E_{j+1}^{n+1} \hat{f}_{j+1/2} + E_{source\ j}^n / \hat{d}_j \tag{22}$$

where we have made several definitions: the source energy in zone j, $E_{source\ j}^n = E_j^n + c\Delta t f_j \sigma_{a\ j} a T_j^{n4}$; the diagonal term of the matrix, $\hat{d}_j$, which is the coefficient of E_j^{n+1} in Eq.(17); the off diagonal term $\hat{f}_{+j} = c\frac{\Delta t}{\Delta x_j}\frac{D_{j+1/2}}{\Delta x_{j+1/2}}/\hat{d}_j$ with $\hat{f}_{-j}$ defined similarly. We also define $E_{total} = \sum_j E_{source\ j}^n$. The symmetry of the matrix is expressed by the fact that $\hat{f}_{+j} = \hat{f}_{-j+1}$ and $\hat{f}_{-j} = \hat{f}_{+j-1}$.

The Monte Carlo solution technique involves some number N of particles associated with the zones of the mesh. The particles are created in the zone j with a probability $E_{source\ j}^n / E_{total}$, carrying energy $E_{particle} = E_{total}/N$. They jump to zone $j+1$ with a probability $P_{+j} \equiv \hat{f}_{+j}/\hat{d}_j$ and zone $j-1$ with a probability $P_{-j} \equiv \hat{f}_{-j}/\hat{d}_j$. When a particle is in zone j, we will tally its energy into E_j^{n+1} with a probability $Pc_j = 1/\hat{d}_j$. We will refer to this event as census, because it will be seen to be analogous to the census event in the IMC algorithm. A particle in zone j can also tally into another variable $E_{absorbed\ j}$ with probability $Pa_j \equiv c\sigma_a \Delta t/\hat{d}_j = 1 - P_{+j} - P_{-j} - Pc_j$. $E_{absorbed\ j}$ will be seen to be the energy absorbed by the matter in zone j. We follow each particle from zone to zone until it tallies into either E_j^{n+1} or $E_{absorbed\ j}$ in some zone, or leaves the problem through the ends. When all the particles tallied, we are through with the time step.

The probabilities we have defined all evidently satisfy the requirement that they be greater than or equal to zero and less than or equal to one, and they all add to one. This is because of the nature of the matrix we have defined. In particular, P_{+j} and P_{-j} satisfy these inequalities because the off-diagonal terms in the matrix were negative, and also

appeared in the diagonal term with positive sign.

We will now show that the expected value of E_j^{n+1}, which we will denote $< E_j^{n+1} >$, obtained by from this algorithm satisfies Eq.(22).

The expected value $< E_j^{n+1} >$ satisfies

$$< E_j^{n+1} >= Pc_j \lim_{N\to\infty} E_{particle} N_j \tag{23}$$

where N_j is the number of particles that pass through the zone j. A particle in zone j must either be born in zone j or jump there from another zone. This implies

$$\lim_{N\to\infty} N_j = P-_{j+1} \lim_{N\to\infty} N_{j+1} + P+_{j-1} \lim_{N\to\infty} N_{j-1} + N_{born},$$

where

$$N_{born} = N_{total} E_{source\ j}/E_{total} = E_{source\ j}/E_{particle}.$$

Using these relations, we obtain

$$< E_j^{n+1} >= Pc_j P-_{j+1} \lim_{N\to\infty} E_{particle} N_{j+1} + Pc_j P+_{j-1} \lim_{N\to\infty} E_{particle} N_{j-1} + Pc_j E_{source\ j}. \tag{24}$$

Using the symmetry of the matrix, the terms involving the products of probabilities can be rewritten:

$$P+_{j-1} = \frac{\hat{f}+_{j-1}}{\hat{d}_{j-1}} = \frac{\hat{f}-_j}{\hat{d}_j}\frac{\hat{d}_j}{\hat{d}_{j-1}} = P-_j\, Pc_j/Pc_{j-1} \tag{25}$$

which leads to $P+_{j-1}\, Pc_j = P-_j\, Pc_j$. Similarly, $P-_{j+1}\, Pc_j = Pc_{j+1} P+_j$.

Using these relations, and the definition of $Pc_j = 1/\hat{d}_j$, we find that

$$< E_j^{n+1} >= P-_j \lim_{N\to\infty} Pcj+1 E_{particle} N_{j+1} + P+_j \lim_{N\to\infty} Pc_{j-1} E_{particle} N_{j-1} + E_{source\ j}/\hat{d}_j. \tag{26}$$

Using the definition of the expected value, this becomes

$$< E_j^{n+1} >= P-_j < E_{j+1}^{n+1} > + P+_j < E_{j-1}^{n+1} > + E_{source\ j}/\hat{d}_j. \tag{27}$$

The expected values for the energy produced by the algorithm satisfy the difference equation Eq.(22) we wish E_j^{n+1} to satisfy. Thus, we can take the results for E_j^{n+1} we get from the random walk, which are obtained with a finite number of particles, as an approximate solution of the equation. Since the E_j^{n+1} represents the photon energy in zone j at time $n+1$, the tally of a photon into E_j^{n+1} is analogous to an IMC particle reaching census. On the next time step, our values E_j^{n+1} become the E_j^n used in the source term.

A similar calculation will show that Eq.(18) can be manipulated to give probabilities that hold in zone 1, and that these give rise to expectation values that satisfy Eq.(18). The probabilities for zone 1 are derived by dividing the equation by the diagonal term, just as they are in the case of Eq.(18). In particular, the value of $P-_1$, the probability that the particle leaves the problem though the boundary at $x = 0$, comes from the term in the denominator that arises from the boundary term, Eq.(15). A similar term arises at

the $x = x_{max}$ boundary. We tally the energy of particles that leave the problem into the variable $E_{escaped}$.

The IMD particles collectively carry E_{total}, and they deposit energy in a conservative way. This implies $\sum_j E_{absorbed\ j} = E_{total} - \sum_j E_j^{n+1} - E_{escaped}$. $E_{absorbed\ j}$, the energy that is not tallied into census, must therefore be the amount of energy that was absorbed by the matter in each zone. This energy is used to solve the matter energy balance Eq.(21), to obtain the new matter temperature T_j^{n+1}.

The algorithm in the 2D case is exactly the same, accept that there are probabilities of jumping to four neighboring zones rather than two. The probabilities of jumping in the 2D case are given by dividing the flux by the diagonal term, just as in the 1D case. Pc and Pa will be given by the same expressions as in the 1D case.

Applying the Monte Carlo solution technique above to the matrix equations produces a very simple, easy to code algorithm with a very physical interpretation, and which resembles IMC very closely. Our Monte Carlo matrix inversion procedure begins by starting some number of particles in each zone. The weight of the particles is the value of the source term in that zone divided by the number of particles. The source term is $E_j^n + c\Delta t f_j \sigma_{a\ j} a T_j^{n4}$. E_j^n is the radiation energy at time n, which corresponds to the photons in census in an IMC calculation, while $c\Delta t f_j \sigma_{a\ j} a T_j^{n4}$ is the energy radiated from the matter in that zone, just as in an IMC calculation. So our particles have weights, interpretable as the energies that IMC particles generated in the zones would have had. We will refer to these particles as IMD particles.

IMD particles are advanced by drawing a random number and comparing it to the probabilities derived from the matrix. The probability of reaching census, i.e., contributing to E_j^{n+1}, is $1/\hat{d}_j$. If this event occurs, the particles energy is tallied into the variable holding E_j^{n+1}. The probability of absorption is $c\Delta t f_j \sigma_{a\ j}$. If this event occurs, the particle's energy is tallied into the variable holding the amount of energy absorbed by the matter in that zone from the radiation field. The probability of jumping to a new zone k is $\hat{f}_{j,k}/\hat{d}_j$, the ratio of the fringe term associated with zone k to the diagonal of the current zone j. If this event occurs, the particle is moved to zone k, a new random number is drawn, and the particle is advanced again using the probabilities from zone k.

As a variance reduction technique, we can use a path length estimator for the census and absorption events, rather than the last event estimator described above. In the last event estimator, we tally all of the energy of the particle into census or absorption if that is the event selected, and stop advancing the particle. In the path length estimator, we tally an amount equal to the probability of census and absorption multiplied by the particles energy on each step. Then we subtract the tallied energy from the particles energy. In this method, the particle continues to move indefinitely with a decreasing energy. To prevent wasting computational resources on particles with small weights, the particle is terminated when the weight reaches some small fraction of the initial weight. We have used .01 of the initial energy as the cutoff in the calculations described in section 5.

IMD, as a Monte Carlo method, produces a solution with statistical noise in it. This can impact the solution of discretized diffusion equations with flux limiters.

As discussed in Szilard and Pomraning (1992) and Olson (2000), flux limiters use some approximation of the slope of the energy to modify the value of diffusion coefficient

D when $|\nabla E|/E$ is comparable to σ. This occurs when σ is small or when the radiation energy is changing rapidly, which is when the diffusion approximation is not applicable. Flux limiters are essentially a way to employ diffusion in regions where a full transport solution would be more appropriate.

The value D is assigned when a flux limiter modifies it depends non-linearly on ∇E. This non-linearity would prevent formulating the discretized diffusion equation as a matrix equation, so t^n values for E are often used. Iteration is also sometimes employed.

When IMD is used to invert the matrix, the statistical noise in the values obtained for E will make the calculation of ∇E used in the flux limiter inaccurate. This makes the IMD algorithm a poor one for solving flux-limited diffusion equations, although one might be able to use it if some kind of smoothing was imposed on the values used to calculate ∇E. IMD is useful when coupled to IMC in a hybrid method. Then IMC can be used where the transport equation is more appropriate (i.e., where a flux limiter would be needed), and IMD can be used where the diffusion approximation is accurate.

In the calculations described in this paper, we have employed the diffusion approximation only in regions with σ so large that a flux limiter would not be expected to modify the value of D. Experimentation confirmed that the flux limiter given above did not modify the value of D obtained from $D = 1/(3\sigma)$. The hybrid results presented in section 5 were not run with a flux limiter in IMD.

Advancing the IMD particles is very similar to advancing IMC particles. They both deposit energy in the matter, and reach census. Their tracking behavior is much simpler, however. IMD particles do not have a position in the zone, a time, or a direction. They are associated with the whole zone, which is because the diffusion equation results from an integration over angles, and the discretization that produced the matrix employed zone and time average quantities.

In a zone with a large real scattering opacity, or a zone in which the induced scattering is large, an IMC particle will perform many scatters. Each scatter is relatively expensive, requiring, among other things, a calculation of the distance from the IMC particle's current location to the zone boundary, the computation of a natural logarithm to determine the distance to a scatter, and several if tests to determine the particles fate. Advancing an IMD particle is much cheaper, because this distance to boundary calculation is not needed, and because the particle always leaves the zone during a step. In effect, many expensive IMC steps can be replaced by one inexpensive IMD step, at the cost of replacing the solution of the transport equation with the solution of the diffusion equation. If the problem is highly scattering, or some regions of it are, we may be willing to make this tradeoff, since the increase in speed my be quite large, while the decrease in accuracy may be tolerable. In the next section, we will describe the IMC/IMD hybrid method. In the section following that, we will demonstrate the IMC/IMD hybrid method on two test problems and examine the tradeoff.

An IMC/IMD hybrid method

Hybrid algorithms, with IMC and diffusion running in the same problem, have been described in the literature (Pomraning and Foglesong, 1979). In these hybrid algorithms, part of the problem is run with IMC, and the highly scattering part, which would be prohibitively expensive to run with IMC, is run with diffusion. Dividing the problem up in this way means selecting the zones in which diffusion is an appropriate approximation, and forming a matrix equation on each contiguous set of these zones. IMC particles are advanced through the zones not selected as diffusion zones.

The similarity of IMD with IMC makes it easy to mate the two. The problem is divided into IMD and IMC regions by identifying zones where the diffusion approximation is acceptable. Since IMC particles are simulating the transport equation, which is accurate even in the diffusive region, we can allow IMC particles to penetrate freely into the these regions. The IMC region does not provide a flux for the diffusion calculation, so no problems involving negative probabilities of reflection result, as arose in (Pomraning and Foglesong, 1979). Since there is no flux into the diffusion region at its boundary, a vacuum boundary condition is imposed there. In the IMC regions, IMC particles are radiated from the matter in the zones at the start of the time step. In the IMD regions, IMD particles are radiated. As IMC particles which penetrate the IMD heat the matter there, it radiates IMD particles in subsequent time steps.

When an IMD particle jumps from a zone in the diffusive region into a zone in the IMC region, it is converted into an IMC particle at the boundary between the zones. The IMC particle thus has an energy equal to that of the IMD particle. A location on the interface between the zones is calculated stochastically, as it would be for a source particle created on that interface by, for example, a temperature source. Similarly, direction cosines are generated from the cosine distribution, and a time between t^n and t^{n+1} is randomly assigned to the particle.

Although the IMC particles will contribute to an accurate solution of the transport equation in regions of high scattering, they are still expensive to track in these regions. We might wish to convert IMC particles to IMD particles to reduce the cost of the calculation. However, they might scatter out after a few steps, and the repeated conversion of IMC to IMD particles and back is expensive. We have found that converting IMC particles in IMD regions to IMD particles after they take 50 IMC steps produces good results with a useful reduction in the runtime.

IMC particles can travel through all zones of the problem within a radius of $c\Delta t$ from their point of origin. IMD particles can, by converting into IMC particles, also travel throughout the problem. Thus, all zones that are causally connected can exchange particles, even if they are in diffusive regions separated by IMC regions. The regions are coupled together implicitly, and there are no stability time step restrictions, only accuracy restrictions.

Numerical Results

We will demonstrate at the IMC/IMD hybrid method produces a result essentially identical to the result of a standard matrix inversion method, differing only in that it has, like all Monte Carlo methods, some statistical noise. We will then demonstrate coupled IMC and IMD method on two problems which possess both opaque and non-opaque regions, for which diffusion alone would be expected to produce an inaccurate answer, and for which IMC alone requires a prohibitively large amount of computational resources.

The first problem is the test problem from (Szilard and Pomraning, 1992). We will compare the output of a pure IMD calculation to the results of a simulation using the difference equations given in this reference and solved with a tridiagonal solver in the standard way. In this test problem, a temperature source at $T_{source} = \sqrt{2}$ at one end of the problem generates a radiation wave which penetrates into an initially cold slab.

The temperature source forms a Marshak wave which proceeds into the material. Figure 1 shows the radiation temperature at 3 different times during the calculation as calculated with IMD and with the method given in (Szilard and Pomraning, 1992). Figure 2 shows the matter temperature. These figures plot the same variables as Figures 1 and 2 in (Szilard and Pomraning, 1992).

Both methods produce almost identical results. In this calculation, IMD was run with 10000 particles. The IMD calculation took considerably longer than the calculation done with the traditional finite difference method. (Both calculations took one minute or less on a 533 MHz. DEC alpha machine.) This is not surprising, as the tridiagonal matrix that the difference method in (Szilard and Pomraning, 1992) uses may rapidly be inverted. Monte Carlo matrix inversions are usually much slower than traditional methods of inverting a matrix (Palmer and Eccleston, 1999). We are interested in the speedup we can attain over IMC calculations on problems for which diffusion cannot be employed everywhere. We will now examine two such problems, comparing pure IMC to the IMC/IMD hybrid method.

The first hybrid problem is a 1D Cartesian problem in which a region with $\sigma_a = .1$ abuts a region with $\sigma_a = 100$. The low opacity region extends from $x = 5$ to $x = 10$ and is headed by a temperature source at $x = 10$ with a constant temperature of $T_{source} = 10$. The high opacity region extends from $x = 0$ to $x = 5$. A vacuum boundary condition is imposed at $x = 0$. The initial temperature in both materials was $T_{initial} = 10^{-3}$, and the heat capacity was $48T^3$. The units were chosen such that $c = a = k = 1$.

In the high opacity region, the scattering fraction = $1 - f = .988$ (independent of temperature), so IMC particles in that region have a very small scattering mean free path. We would expect that IMC would be very expensive in the high opacity region and that diffusion would be inaccurate in the low opacity region.

The problem has an approximate steady state solution. In the steady state, $E_m = E = T^4$. The temperature in the low opacity region will approach $T_{source} = 1$. In the low opacity region, the radiation and the matter will reach equilibrium. The matter and radiation

energy densities will be equal and satisfy the time independent diffusion equation

$$-\frac{\partial}{\partial x}\left[D\frac{\partial E}{\partial x}\right]=0 \tag{28}$$

on $0 < x < 5$, with $E = 1$ at $x = 5$ and $D = 1/300$. A vacuum boundary condition is imposed at $x = 0$:

$$E_{x=0} + 2D\frac{\partial E}{\partial x}|_{x=0} = 0. \tag{29}$$

This has the solution:

$$E(x) = \frac{x+2D}{5+2D} \tag{30}$$

for $0 < x < 5$

The problem was run with 110 zones, with zoning of $\Delta x = 1$ for $0 < x < 4$ and $5 < x < 10$. In $4 < x < 5$ there were 20 zones with geometrically decreasing size, with the largest zone spaning the region $x = 4$ to $x = 4.0928033856$. $\Delta t = 10$, and the problem was run to $t = 50000$. This was considered to be steady state by comparison with the solution at $t = 100000$, which was essentially the same as the one at $t = 50000$. The IMC calculation was run with 5000 particles per time step. In the hybrid simulation, the sum of the number of IMC and IMD particles was 5000 in each time step. These were apportioned between IMC and the IMD in the same ratio as the sum of source and census energy of the IMC and IMD particles.

Figure 3 shows matter temperature for simulations run with pure IMC, and one with a hybrid method with IMC particles run everywhere, and IMD particles run in the high opacity region $0 < x < 5$. Both methods show good agreement with the approximate analytic answer, which is also shown.

The pure IMC calculation took 21642 seconds, and the hybrid method took 504 seconds, giving a speedup of approximately a factor of 43. Both calculations were run on 533 MHz DEC alpha chip.

Figure 4 shows a plot of the number of particle steps taken by both methods. The pure IMC method takes most of its steps in the high opacity region, which spans zones 1 to 60. In the hybrid calculation, many fewer IMC steps were taken in the high opacity region. Since each IMC step takes about the same amount of computer time, and the IMC steps are more expensive than the IMD steps, the time of each simulation is approximately proportional to the area under the curve representing the number of IMC steps taken. Thus the speedup of greater than 40 times is understandable as a result of the fact that so many fewer IMC steps were taken in the high opacity material.

The second problem is a 2D problem developed by Frank Graziani and often referred to as the tophat problem (Graziani, 2000). In this problem a cylindrical section of material with mass density $\rho = 0.01\ g/cm^3$ and $\sigma_a = 0.2\ cm^{-1}$ is embedded in thick material with $\rho = 10\ g/cm^3$ and $\sigma_a = 2000\ cm^{-1}$. The heat capacity $c_v = 10^{15}\ erg/g - keV$ for both materials. A temperature source with $T_{source} = 0.5\ keV$ is applied at one end of the thin material. Vacuum boundary conditions are applied at all other boundaries. The initial

temperature $T_{initial} = 0.05keV$ everywhere. Time units are such that $c = 300$. The time step begins at $\delta t = 10^{-3}$ and is increased by a factor of 1.1 each time step until it reaches 1.0, and is held constant at 1.0 thereafter.

This problem cannot be run accurately with diffusion alone because diffusion cannot accurately model the flow of radiation around the corners. There is no analytic answer for the problem; the usual figures of merit are the matter temperature at five points in the optically thin material (consult Graziani (2000) for details.)

As time proceeds in this problem, radiation travels down the thin material and around the section of thick material in the middle of the problem, and the thick material slowly heats up. It is in the heated parts of the thick regions that IMC will be most computational intensive. Therefore, we expect that the ratio of the run time of the hybrid calculation to the run time of the pure IMC calculation to diminish as the problem is run farther in time.

This expected result does occur. A problem time of 10, the hybrid calculation took 5483 seconds, while the pure IMC calculation took 34400 seconds, giving a speedup of 6.3. At $t = 100$, the hybrid calculation took 24203 seconds, and the Pure IMC took 573428 seconds, giving a speedup of 23.7. All simulations were run on a 533 MHz DEC alpha.

In Figure 5 we have plotted matter temperature at the five fiducial points from the hybrid simulation and the pure IMC calculation, as well as an Sn solution (Nowak and Nemanic, 1999) Both Monte Carlo calculations had 500,000 total particles per time step. We see good agreement between all three simulations for all the points at most times. Not all points for the hybrid one are shown.

The only notable area of disagreement in this plot is in the behavior of the point farthest from the heat source. In the Sn simulation there is a small decrease in the temperature at this point before the radiation wave begins to heat it. This does not occur in either Monte Carlo simulation. This disagreement occurred because the IMC and hybrid calculations were run with a variance reduction technique; particles were not allocated to zones that were still at the initial temperature. The zone farthest from the heat source, which is near the end of the problem, could actually cool off slightly before the radiation wave reached it. The Sn calculation captured this transient, while the Monte Carlo calculations did not, although they could have if that zone had been allowed to radiate. As soon as the radiation reaches that zone, the effect of the cooling is quickly rendered unnoticeable, and all three simulations show good agreement for this point thereafter.

Figure 6 shows a contour plot of the matter temperature in the problem at $t = 10$. The top half shows the hybrid calculation, while the bottom shows the reflected results of the pure IMC calculation. (Note that these are two separate calculations, whose results have been placed on the same plot by mapping the pure IMC results to "negative" radius.) At this time, the lowest temperature contour of the hybrid calculation slightly lags the pure IMC calculation, but the agreement is otherwise good. The contour lines were manually selected at values between 0.5 and 0.05 so that interesting features in the flow would be highlighted (i.e., flow around corners.)

Figure 7 shows a similar contour plot at $t = 100$. The hybrid calculation shows a slightly greater heating in the thick material, but the agreement in the thin material is very good, and the overall accuracy seems adequate.

We believe the excess heating in the thick material to result from the fact that the

diffusion approximation is not accurate in the cold, thick material, because the scattering opacity is small while the material is cold. The factor f given by Eq.(4) is approximately 1 until the material heats up. A more accurate way of using the hybrid algorithm would be to use IMD only in zones with small f, rather than in zones with a large opacity.

Summary

We have developed a method for increasing the speed of certain IMC radiation transport calculations, which contain regions where the opacity is large. This method employs a Monte Carlo method of matrix inversion to solve the diffusion equation. We have dubbed the method Implicit Monte Carlo diffusion, which we abbreviate IMD. The IMD method employs particles which resemble the particles used in the IMC radiation transport method. Because of this resemblance, the two methods can easily be combined into a hybrid method, where IMD is used in optically thick parts of the problem, where the diffusion approximation provides an accurate approximation to the results of the transport equation. Since the IMD method is considerably faster than the IMC method in these regions, the hybrid method can run much faster than IMC alone on some problems. We have demonstrated this method on 1D Cartesian and 2D cylindrical orthogonal mesh calculations. Test problems on these meshes show that the hybrid method is accurate and can provide speed ups of greater than an order of magnitude. Future work will include extending the method to 3D unstructured grids, and to problems with frequency dependent opacities.

B. R. Eccleston and T. S. Palmer, *Trans. Am. Nuc. Soc.* 81, 148 (1999)

J. A. Fleck, Jr., in "Computational Methods in the Physical Sciences" (B. Alder and S. Fernbach, Eds.) Vol. 1, p.43, McGraw-Hill, New York, 1963

J. A. Fleck, Jr. and J. D. Cummings, *J. Comput. Phys.* 8, 313 (1971)

Graziani F., UCRL document in preparation

Edward W. Larsen, *Ann. Nucl. Ener.* 7, 249 (1980)

Nowak, P., Nemanic, M.,*Proceedings of the ANS Conference on Mathematics and Computation, Reactor Physics and Environmental Analysis in Nuclear Applications*, Madrid, Spain, 1999, pp. 379-390.

Gordon. L. Olson, Lawrence H. Auer, and Michael L. Hall, *J. Quant. Spectros. Radiat. Transfer* 64, 619 (2000)

G.C. Pomraning, *Equations of Radiation Hydrodynamics*, in International Series of Monographs in Natural Philosophy, edited by D. ter Harr (Pergamon, New York, 1973), Vol. 54

G. C. Pomraning and G. M. Foglesong, *J. Comput. Phys.* 32, 420 (1979)

Press, Teukolsky, Vetterling, and Flannery, *Numerical Recipes, Second Edition* (Cambridge University Press, New York, 1992)

R. H. Szilard and G. C. Pomraning, *Nucl. Sci. Engng.* 112, 256 (1992)

This work was performed under the auspices of the U.S. Department of Energy by the University of California Lawrence Livermore National Laboratory under contract No.

W-7405-Eng-48.

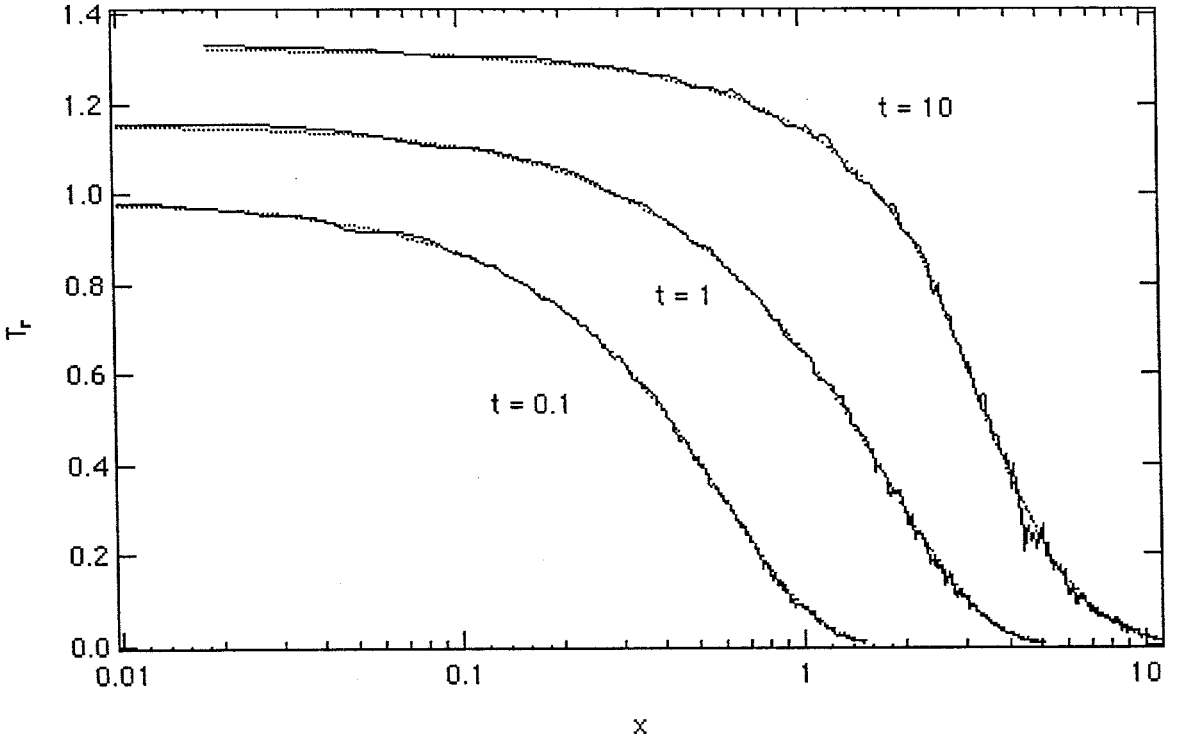

Figure 1: T_r vs. x for t = 0.1, 1.0, and 10. Line: IMD. Dotted: Finite Difference.

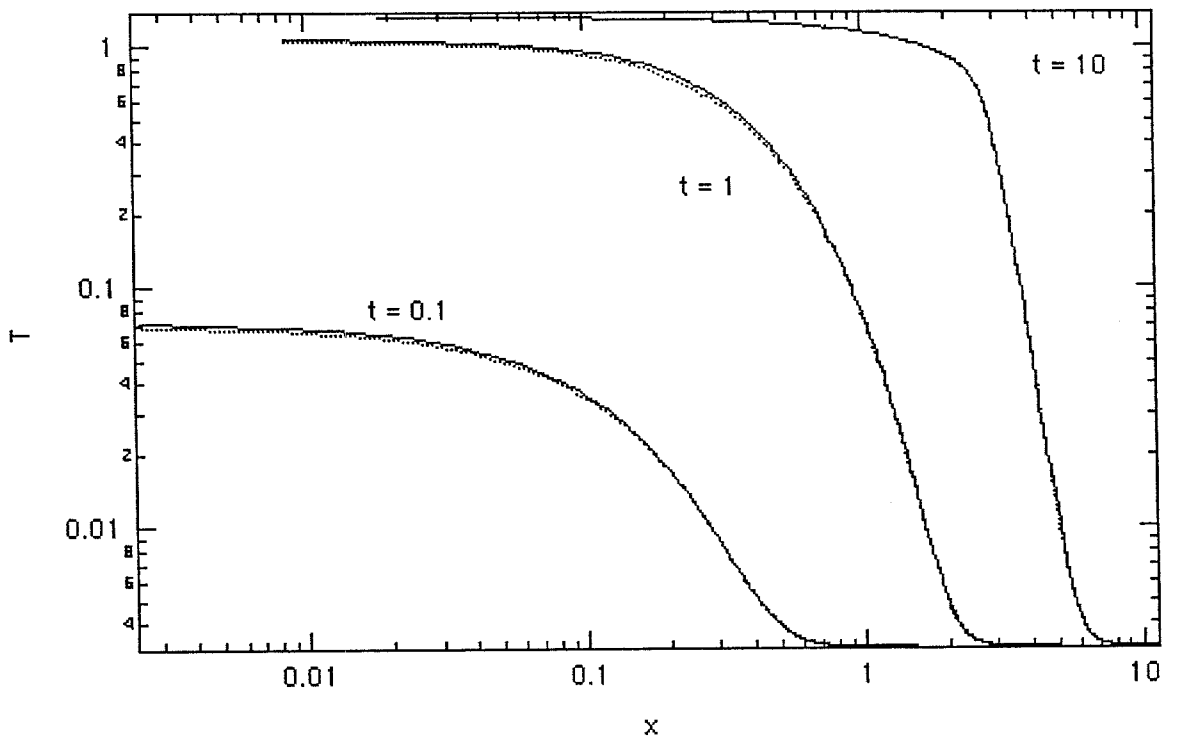

Figure 2: T vs. x for t = 0.1, 1.0, and 10. Line: IMD. Dotted: Finite Difference.

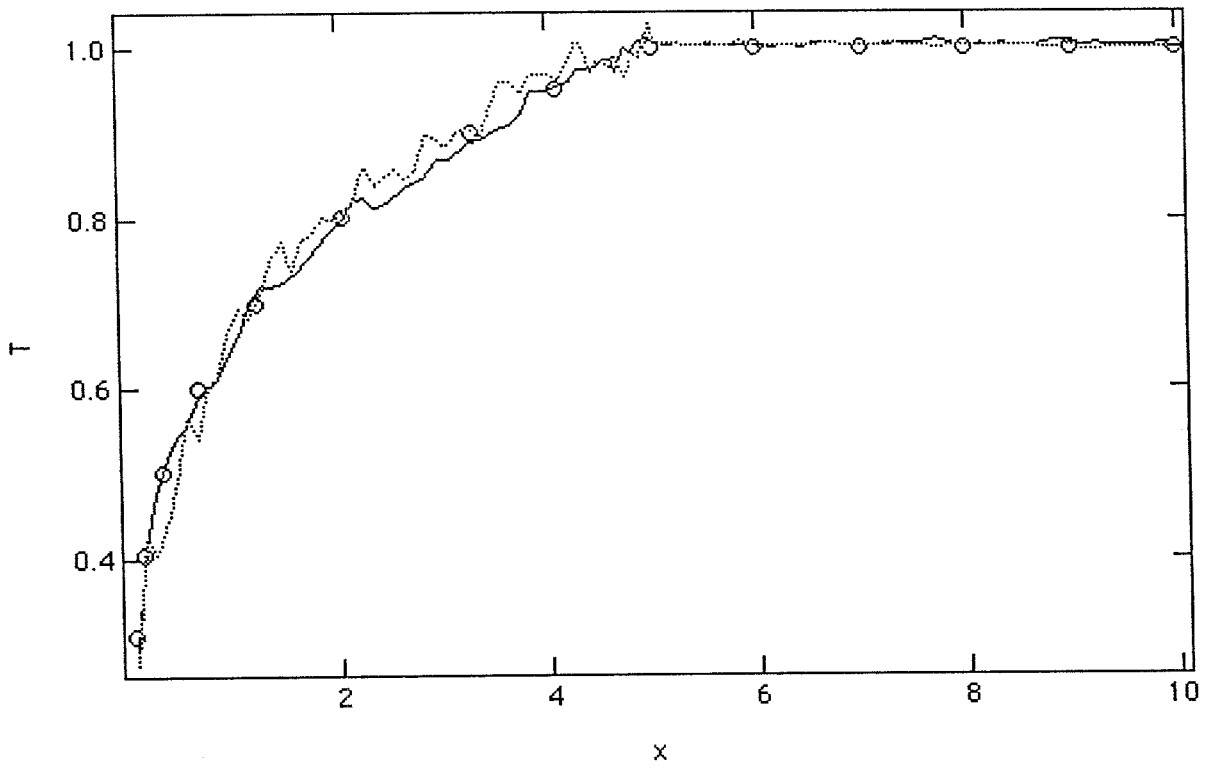

Figure 3: T vs. x at t = 50000 for 1D Cartesian test problem. Circles: analytic result. Dotted: IMC. Line: IMC/IMD hybrid.

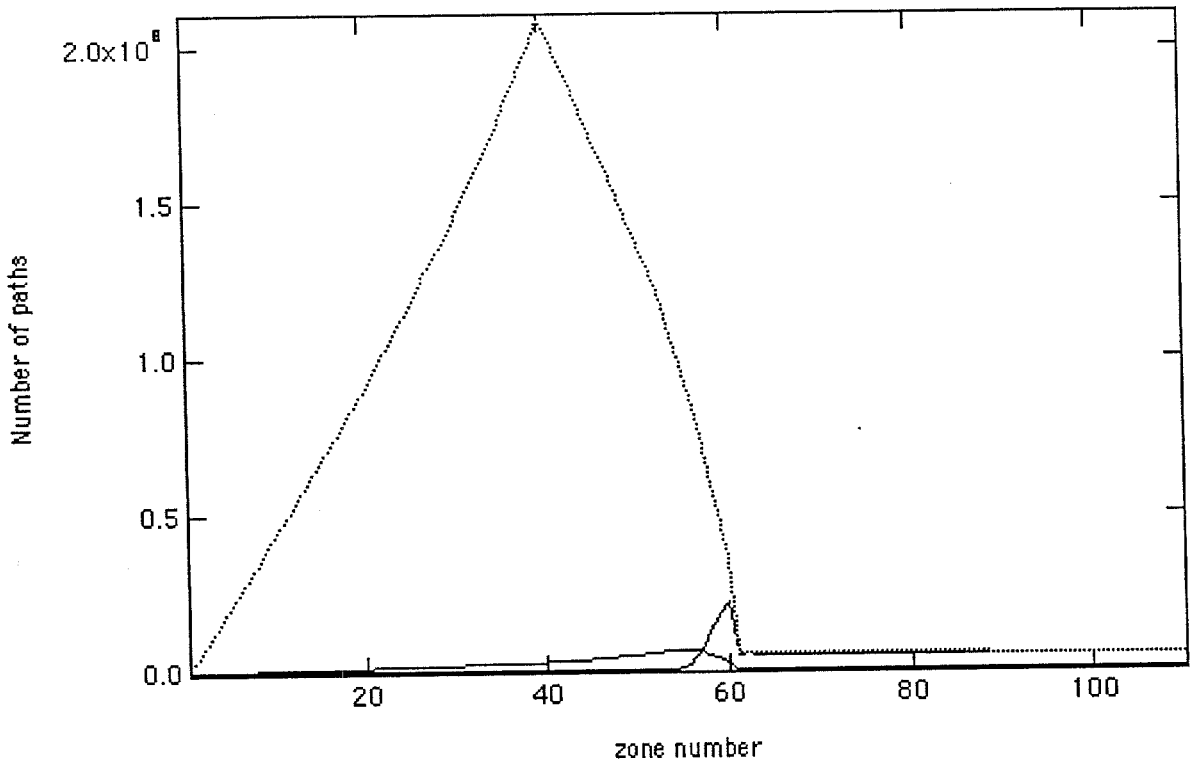

Figure 4: Number of particle paths vs. zone number for 1D Cartesian test problem. Dotted: IMC. Line IMC in hybrid, IMD in hybrid.

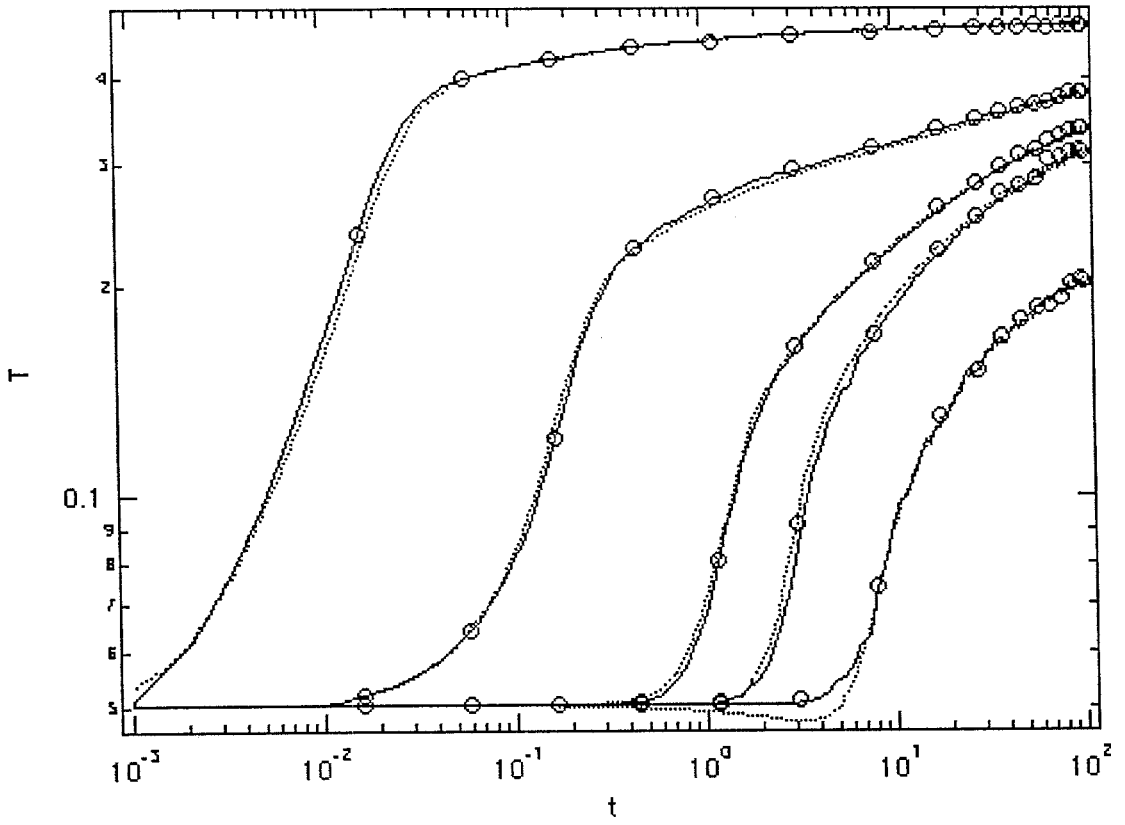

Figure 5: T vs. t for tophat problem. Lines:IMC. Circles: IMC/IMD hybrid. Dotted: Sn

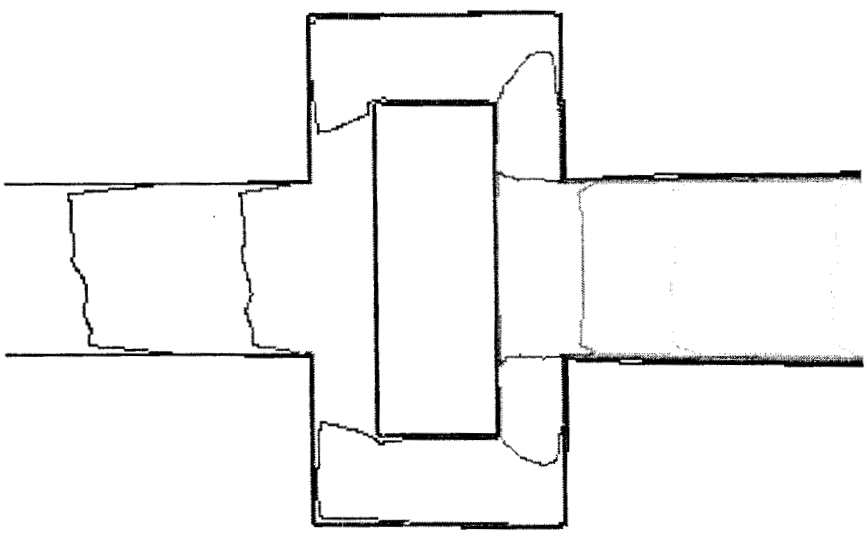

Figure 6: T at t = 10 for tophat problem. Top: IMC/IMD hybrid. Bottom: IMC.

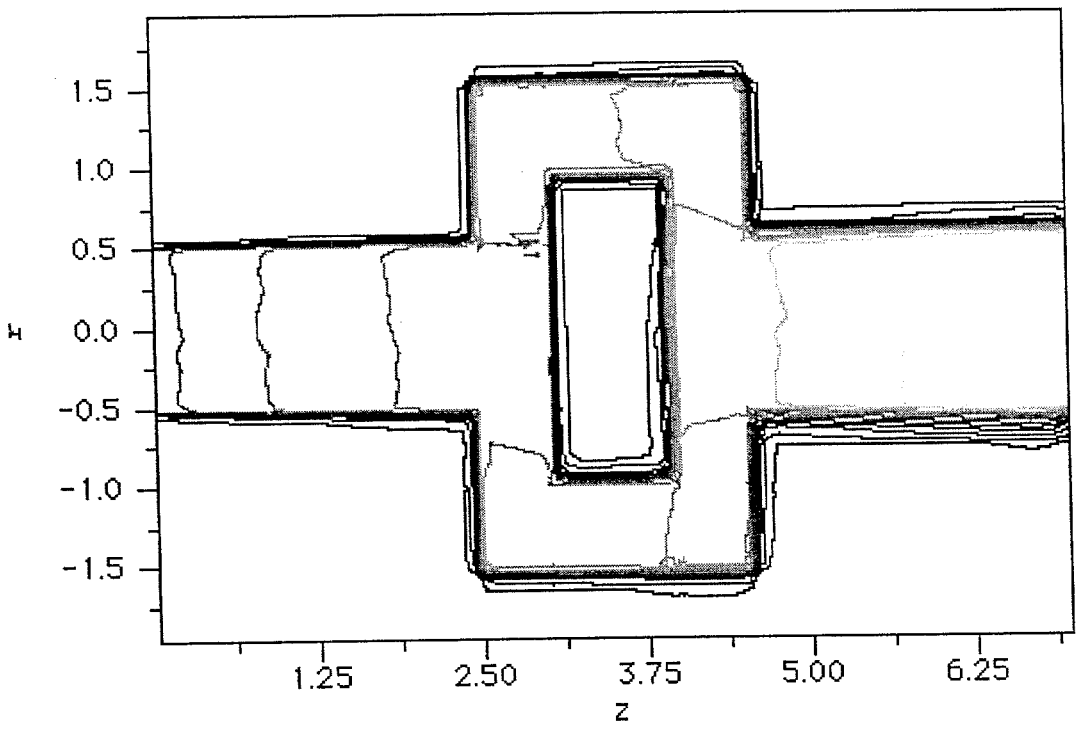

Figure 7: T at t = 100 for tophat problem. Top: IMC/IMD hybrid. Bottom: IMC only.